Numerical Methods for Hyperbolic Equations – Vázquez-Cendón et al. (eds)
© 2013 Taylor & Francis Group, London, ISBN 978-0-415-62150-2

Simulation of an epidemic model with nonlinear cross-diffusion

Stefan Berres
Departamento de Ciencias Matemáticas y Físicas, Facultad de Ingeniería, Universidad Católica de Temuco, Chile

Ricardo Ruiz-Baier
Modeling and Scientific Computing CMCS-MATHICSE-SB, École Polytechnique Fédérale de Lausanne, Switzerland

ABSTRACT: A spatially two-dimensional epidemic model is formulated by a reaction-diffusion system. The spatial pattern formation is driven by a cross-diffusion corresponding to a non-diagonal, upper-triangular diffusion matrix. Whereas the reaction terms describe the local dynamics of susceptible and infected species, the diffusion terms account for the spatial distribution dynamics. For both self-diffusion and cross-diffusion nonlinear constitutive assumptions are suggested. To simulate the pattern formation two finite volume formulations are proposed, which employ a conservative and a non-conservative discretization, respectively. Numerical examples illustrate the impact of the cross-diffusion on the pattern formation.

1 INTRODUCTION

The knowledge of spreading dynamics of infectious diseases helps to design prevention measures. A generic model category for the quantitative description of the epidemic evolution dynamics by an ordinary differential equation are the so-called SIR models, which classify a population into 'susceptible' (S), 'infected' (I) and 'recovered' (R) subgroups and balance the changes between these. One very early and simple prototype of a SIR-model is due to Kermack and McKendrick 1927. It describes the population evolution by the system of ordinary differential equations

$$\frac{dS}{dt} = -\alpha SI, \quad \frac{dI}{dt} = \alpha SI - \beta I, \quad \frac{dR}{dt} = \beta I,$$

where $\alpha > 0$ is the infection rate and $\beta > 0$ the recovery rate. There are several suggestions for improving the specification of these ODE-dynamics (Kim et al. 2010, Li et al. 2010), and structural modifications like SIR-models in networks (Liu & Zhang 2010). A key issue in epidemic modeling is the formation of spatial patterns. Based on a general setting in the two-dimensional reaction-diffusion framework for epidemic processes (Webb 1981), there are several suggestions for the combination of the system of ordinary differential equations of the SIR-model with a spatially two-dimensional diffusion equation of the involved variables (He & Stone 2003, Milner & Zhao 2008, Li & Zou 2009, Sun et al. 2009). Moreover, several contributions have been proposed to study pattern formation induced by cross-diffusion (Ni 2004, Bendahmane et al. 2009b, Tian et al. 2010). In addition to a fundamental existence proof for general reaction-diffusion systems (Crandall et al. 1987), there are several approaches to analyze reaction-diffusion equations with one single "cross-diffusion" that lead to a system with upper triangular diffusion matrix (Badraoui 2006, Daddiouaissa 2008). The structure of an upper triangular diffusion matrix has also been utilized in the existence analysis for systems of convection-diffusion equations with both Dirich-let and Neumann boundary conditions (see e.g. Frid & Shelukhin 2004, Frid & Shelukhin 2005, Berres et al. 2006). Besides numerous contributions to the development of numerical methods to solve reaction-diffusion equations in related contexts (Wong 2008, Phongthanapanich & Dechaumphai 2009), convergence proofs of associated finite volume schemes (Bendahmane & Sepúlveda 2009, Andreianov et al. 2011) and finite element formulations (Galiano et al. 2003, Barrett & Blowey 2004) have been provided.

This contribution is a condensed version of Berres & Ruiz-Baier 2011. The goal is, on the one hand, to generate pattern formation in an epidemic model by a cross-diffusion term, and, on the other hand, to prevent blow-up by a nonlinear limitation of the cross-diffusion. These assumptions are designed to qualitatively reflect psychological behavior. The cross-diffusion term has the interpretation that the susceptible population moves away from increasing gradients of the

infected population. In addition, it is assumed that the cross-diffusion effect depends on the local population density. For the nonlinear cross-diffusion it is assumed that there exists *carelessness* at a small and *fatalism* at a high total population number. At carelessness and fatalism the susceptible population decreases its tendency to avoid agents of the infected population. Such an avoidance is most effective for intermediate (neither too small nor too large) population numbers.

2 CONCEPTUAL MODEL

The two-dimensional reaction-diffusion system describing spatial epidemic dynamics with cross diffusion is written as

$$\begin{aligned} u_t &= f(u,v) + \nabla\cdot\big(a(u)\nabla u\big) + \nabla\cdot\big(c(u,v)\nabla v\big), \\ v_t &= g(u,v) + \nabla\cdot\big(b(v)\nabla v\big), \end{aligned} \tag{1}$$

in $\Omega_T = \Omega\times(0,T)$, where u and v denote the populations of susceptible and infected persons, respectively. No external input is imposed, therefore on the physical domain boundary $\delta\Omega$ the Neumann boundary condition is assumed to hold:

$$(a(u)\nabla u + c(u,v)\nabla v)\cdot n = 0, \quad (b(v)\nabla u)\cdot n = 0,$$

where n is the outer normal vector to the physical domain boundary. In the system (1), an additional equation for the recuperated population is omitted because the model does not consider their feedback on the susceptible or infected population. With the notation

$$u = \begin{pmatrix} u \\ v \end{pmatrix}, \quad f(u) = \begin{pmatrix} f(u,v) \\ g(u,v) \end{pmatrix}, \quad a(u) = \begin{pmatrix} a(u) & c(u,v) \\ 0 & b(v) \end{pmatrix},$$

the system (1) can be written in compact form as

$$\frac{d}{dt}u = f(u) + \nabla\cdot\big(a(u)\nabla u\big).$$

The model enforeces phase separation since the susceptible species avoid the infected population by a cross-diffusion term $\nabla\cdot(c(u,v)\nabla v)$. The cross-diffusion term directs the flow in the opposite direction of the gradient ∇v. Whenever there is an increase of the amount of the infected population then the susceptible aents move away from the direction of the increasing gradient.

The reaction terms are considered to be given by the following specifications (see e.g. Su et al. 2009)

$$\begin{aligned} f(u,v) &= ru(1-u/K) - \beta\frac{uv}{u+v}, \\ g(u,v) &= \beta\frac{uv}{u+v} - kv, \end{aligned} \tag{2}$$

where the model parameters are the carrying capacity of the susceptible species K, r is the intrinsic birth rate, β is the rate of disease transmission, and k represents the recovery rate of the infected species.

The equilibrium points are pairs (u,v) such that $f(u,v) = 0$ and $g(u,v) = 0$. For (2), the equilibrium points are (0,0) (trivial equilibrium), (K,0), which corresponds to the disease-free point, and (u^*,v^*), which corresponds to an endemic stationary state that is explicitly given by

$$(u^*, v^*) = \left(\frac{K(r-\beta+k)}{r}, \frac{K(r-\beta+k)(\beta-k)}{rk}\right).$$

In Figure 1, the phase portrait of the ODE system associated to (1), (2). From now on, as model variants we will consider diffusion terms which are linear (Model 1) and nonlinear (Model 2). For better comparison, in Model 2 the same reaction kinetics (2) as for Model 1 are used.

For Model 1 the diffusion terms are given by the constants

$$a(u) = a_0, \quad b(v) = b_0, \quad c(u,v) = c_0, \tag{3}$$

which adopts the setting of Sun et al. 2009. In Model 2 we propose nonlinear model variants of the parametric functions. The self-diffusion terms are chosen as

$$a(u) = a_0u^m, \quad b(v) = b_0v^m. \tag{4}$$

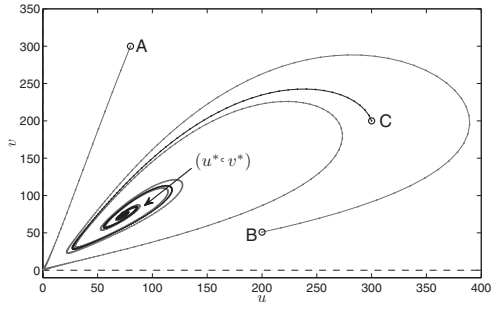

Figure 1. Phase portrait for the ODE system associated to (1), (2). Three trajectories are displayed starting from the states $A = (80,300)$, $B = (200,50)$ and $C = 300,200)$ and reaching the equilibrium point (u^*, v^*). The parameters correspond to those used in Example 1.

By the assumption that $m \in (-1,0)$, a degressive growth is described since

$$\partial_u a(u) < 0, \quad \partial_v b(v) < 0 \quad \text{for all} \quad u,v.$$

The biological interpretation is that the tendency to avoid crowds reduces with higher numbers as the population "gets used" to them. Using the notation of the Laplace operator,

$$\Delta A(u) = \nabla \cdot \big(a(u)\nabla u\big), \quad \Delta B(v) = \nabla \cdot \big(b(v)\nabla v\big), \qquad (5)$$

we have

$$A(u) = \frac{a_0}{m+1} u^{m+1}, \quad B(v) = \frac{b_0}{m+1} v^{m+1}, \qquad (6)$$

where $A(u)$ and $B(v)$ are sub-linear functions. For $m = 0$ the functions (4) of Model 2 boil down to those of the linear Model 1 (3) as

$$A(u) = a_0 u, \quad B(v) = b_0 v.$$

The construction of a conservative or nonconservative discretization depends roughly speaking on whether the finite differences are based on the formulation of the left-hand or right-hand side of (5), respectively.

A nonlinear cross-diffusion function implements a situation-dependent tendency of the susceptible population to avoid the infected population. This situation-dependent behavior reflects an average psychological disposition. An approach to model such a disposition is as follows. From the perspective of the susceptible population, avoidance is pursued whenever there is an awareness, i.e., when there is a detectable fraction of the infected population. For a small number of populations the necessary awareness has not been matured or is temporarily not active, since then there is no vital urgency for self-protection. In the other extreme, at large population numbers, such a selective detection is neither possible nor makes sense, since there is less, or even no chance to avoid infection in the crowd. The population number affects the conscious disposition of avoidance. Therefore, the cross-diffusion coefficient is designed to be negligible for imposed by the following constraints both small and large number of populations, which is imposed by the following constraints

$$c(u,0) = 0, \quad c(0,v) = 0, \quad \text{for all} \quad u,v \in \mathbb{R},$$
$$c(u,v) = 0 \quad \text{for} \quad v \geq V(u),$$

where V is a Lipschitz continuous monotonically decreasing function with a zero for $u > 0$. For example, one might choose $V(u) = c_1 - u$ with $c_1 > 0$. By these constraints, the reaction-diffusion equation with cross-diffusion (1) degenerates into an equation without cross-diffusion outside the domain

$$\tilde{\Omega} := \big\{(u,v) : u,v \geq 0,\, v < V(u)\big\}.$$

The constraints (7) are satisfied, for example, by a function which is quadratic in the domain $u,v \geq 0,\ u + v = c_1$

$$c(u,v) = c_0 uv(c_1 - u - v), \quad c_0, c_1 > 0, \qquad (8)$$

and vanishes ($c(u,v) = 0$) otherwise. This quadratic function is convex and takes its global maximum in

$$(\hat{u},\hat{v}) = \left(\frac{c_1}{3}, \frac{c_1}{3}\right). \qquad (9)$$

In the sequel some supporting arguments for the constraints (7) and in particular for the nonlinear model (8) are summarized. First of all, the constraint $c(u,0) = 0$ for all v corresponds to carelessness; during the absence, and also in the case of a small number of infected persons, the consciousness of the danger of the disease is not sufficiently present, even though there might be are some single dangerous intercourses. The constraint $c(0,v) = 0$ for all u is not only set for symmetry reasons, since, at a small number of susceptible agents, they have little chance to form a group consciousness on the importance of a separation from the infected population; instead, the susceptible population is absorbed by the infected population. The maximum $(\hat{u},\hat{v})$ has the interpretation that there is most avoidance when there is a fairly equal mixing of susceptible and infected population, whereas at small population numbers there is less need and at large total population numbers no possibility for avoidance.

In the situation of a large concentration of persons there is little possibility of a selective avoidance. Since the infected species is present anywhere and thus cannot be sustainably avoided in the crowd, there is small to no possibility to keep distance from the infected species. Thus, fatalism rules above a certain threshold 'upper' population number. This fatalism is modelled by the assumption that the cross-diffusion coefficient vanishes above this threshold population number. This upper population bound is set by the function V such that c_1 corresponds to a maximum population, where, in the case that $c_1 = u + v$, total fatalism rules.

A formal property of the constraints (7) is the that the cross-diffusion is switched off at a certain finite total population. By this setting, it is

prevented that the population attains (unrealistic) local population peaks. In fact, by this limitation of the cross-diffusion, a maximum principle for the system (1) is imposed. The switch-off of the diffusion term can be seen in the context of equations with strongly degenerate diffusion, where the diffusion function is set to zero on an interval as proposed in (Bürger & Ruiz-Baier 2009, Bürger et al. 2010).

3 NUMERICAL ANALYSIS

In order to provide a space-adaptive numerical scheme, we apply the technique of fully adaptive multiresolution (Bendahmane et al. 2009a, Bürger et al. 2010) constructed on the basis of a reference finite volume approximation (Eymard et al. 2000, see also e.g. Müller 2003 for a survey on multiresolution methods for PDEs). The success of this approach mainly relies on the strategy used for storing only the relevant information. The numerical approximation obtained in each time step is represented (and also computed) using a dynamically evolving adaptive mesh which is generated from a sequence of nested grids. An appropriate smoothness analysis of the solution is performed using wavelet decomposition and such information on the local smoothness is used to locally adapt the mesh and the numerical scheme. Essentially, positions related to small wavelet coefficients may be discarded, allowing for substantial data and CPU-time compression.

Admissible rectangular meshes

These ideas are made precise, first by introducing a nested hierarchy of grids $T^0 \subset \cdots \subset T^H$, where each grid T^ℓ, $\ell = 0, \ldots, H$ is assumed to be an *admissible rectangular mesh*. The index $\ell = 0$ corresponds to the coarsest and $\ell = H$ to the finest resolution level, which is fixed and chosen large enough at the beginning of the algorithm. That is, a partition of Ω formed by control volumes K^ℓ (open rectangles of maximum diameter h_{K^ℓ}), constrained by the condition that the segment joining the centers of two neighboring control volumes x_{K^ℓ} and x_{L^ℓ} must be orthogonal to the corresponding interface $\sigma = \sigma(K^\ell, L^\ell)$. The interface length is denoted by $|\sigma| = |\sigma(K^\ell, L)|$. By $\varepsilon(K^\ell)$ we denote the set of edges of K^ℓ, $\varepsilon_{\text{int}}(K^\ell)$ corresponds to those is in the interior of T^ℓ and $\varepsilon_{\text{ext}}(K^\ell)$ is the set of edges of K^ℓ lying on the boundary $\partial\Omega$, i.e.,

$$\varepsilon\left(K^\ell\right) = \varepsilon_{\text{int}}\left(K^\ell\right) \cup \varepsilon_{\text{ext}}\left(K^\ell\right),$$
$$\varepsilon_{\text{int}}\left(K^\ell\right) \cap \varepsilon_{\text{ext}}\left(K^\ell\right) = \varnothing \quad \text{for all } K^\ell \in T^\ell.$$

By $\varepsilon^\ell_{\text{int}}$ and $\varepsilon^\ell_{\text{ext}}$ we will denote the sets of all edges in the interior of T^l and lying on the boundary $\partial\Omega$, respectively. For a given finite volume K^ℓ, we denote by $N(K^\ell)$ the set of neighbors of K^ℓ which share a common edge with K^ℓ. For all $L^\ell \in N(K^\ell)$, $d(K^\ell, L^\ell)$ denotes the distance between x_{K^ℓ} and x_{L^ℓ}.

Two one-level finite volume methods

In order to define the discrete marching formula for (1), we choose an admissible discretization of Ω_T consisting of an admissible mesh T^l of Ω and a time step size $\Delta t > 0$. We may choose $N > 0$ as the smallest integer such that $N\,\Delta\, t \geq T$, and set $t^n := n\,\Delta\, t$ for $n \in \{0,\ldots,N\}$.

We denote the cell averages of u and v on $K^\ell \in T^\ell$ at time $t = t^n$ by the respective expressions

$$u^n_{K^\ell} := \frac{1}{\left|K^\ell\right|}\int_{K^\ell} u\left(x, t^n\right) dx,$$
$$v^n_{K^\ell} := \frac{1}{\left|K^\ell\right|}\int_{K^\ell} v\left(x, t^n\right) dx.$$

Furthermore, we define the coefficients

$$f^n_{K^\ell} := f\left(u^n_{K^\ell}, v^n_{K^\ell}\right), g^n_{K^\ell} := g\left(u^n_{K^\ell}, v^n_{K^\ell}\right),$$
$$a^n_{K^\ell} := a\left(u^n_{K^\ell}\right), b^n_{K^\ell} := b\left(v^n_{K^\ell}\right),$$
$$c^n_{K^\ell} := c\left(u^n_{K^\ell}, v^n_{K^\ell}\right).$$

For constant coefficient functions (3) one has an $a^n_{K^\ell} = a_0, b^n_{K^\ell} = b_0, c^n_{K^\ell} = c_0$ on all cells K^l and time steps n. The computation starts from the initial cell averages

$$u^0_{K^\ell} = \frac{1}{\left|K^\ell\right|}\int_{K^\ell} u_0(x)\, dx, \quad v^0_{K^\ell} = \frac{1}{\left|K^\ell\right|}\int_{K^\ell} v_0(x)\, dx.$$

The resulting finite volume scheme for the approximation of (1), defined on the multiresolution level l assumes values $u^n_{K^\ell}$ and $v^n_{K^\ell}$ for all $K^\ell \in T^\ell$ at time $t = t^n$ and determines $u^{n+1}_{K^\ell}$ and $v^{n+1}_{K^\ell}$ for all $K^\ell \in T^\ell$ at time $t = t^{n+1} = t^n + \Delta t$ by a marching formula. For linear coefficients (3) the system (1) is discretized as

$$\left|K^\ell\right| \frac{u^{n+1}_{K^\ell} - u^n_{K^\ell}}{\Delta t} =$$
$$\left|K^\ell\right| f^n_{K^\ell} + \sum_{\sigma \in \varepsilon_{\text{int}}\left(K^\ell\right)} \frac{\left|\sigma\left(K^\ell, L^\ell\right)\right|}{d\left(K^\ell, L^\ell\right)} \left\{ a_0\left(u^n_{L^\ell} - u^n_{K^\ell}\right) + c_0\left(v^n_{L^\ell} - v^n_{K^\ell}\right)\right\},$$

$$\left|K^\ell\right|\frac{v_{K^\ell}^{n+1}-v_{K^\ell}^n}{\Delta t}=$$
$$\left|K^\ell\right|g_{K^\ell}^n+\sum_{\sigma\in\varepsilon_{\text{int}}\left(K^\ell\right)}\frac{\left|\sigma\left(K^\ell,L^\ell\right)\right|}{d\left(K^\ell,L^\ell\right)}b_0\left(u_{L^\ell}^n-u_{K^\ell}^n\right). \tag{10}$$

This marching formula is valid for all cells and in particular for the boundary cells. The no-slip boundary condition is considered automatically by not considering boundary fluxes, such that they are automatically set to zero.

For nonlinear coefficient functions the generalization of (10) is not uniquely determined. Therefore, two versions are suggested, which are denoted by scheme A and scheme B, respectively. Scheme A has the form

$$\left|K^\ell\right|\frac{u_{K^\ell}^{n+1}-u_{K^\ell}^n}{\Delta t}=\left|K^\ell\right|f_{K^\ell}^n+$$
$$\sum_{\sigma\in\varepsilon_{\text{int}}\left(K^\ell\right)}\frac{\left|\sigma\left(K^\ell,L^\ell\right)\right|}{d\left(K^\ell,L^\ell\right)}\left\{\frac{\left(a_{L^\ell}^n+a_{K^\ell}^n\right)}{2}\left(u_{L^\ell}^n-u_{K^\ell}^n\right)+\right.$$
$$\left.\frac{2c_{K^\ell}^nC_{L^\ell}^n}{C_{K^\ell}^n+C_{L^\ell}^n}\left(v_{L^\ell}^n-v_{K^\ell}^n\right)\right\},$$
$$\left|K^\ell\right|\frac{v_{K^\ell}^{n+1}-v_{K^\ell}^n}{\Delta t}=\left|K^\ell\right|g_{K^\ell}^n+$$
$$\sum_{\sigma\in\varepsilon_{\text{int}}\left(K^\ell\right)}\frac{\left|\sigma\left(K^\ell,L^\ell\right)\right|}{d\left(K^\ell,L^\ell\right)}\frac{\left(b_{L^\ell}^n+b_{K^\ell}^n\right)}{2}\left(v_{L^\ell}^n-v_{K^\ell}^n\right). \tag{11}$$

Whereas the coefficient functions $a(u,v)$ and $b(u,v)$ are averaged, for the coefficient function $c(u,v)$ the exchange coefficient in the cross-diffusion term is computed by the following harmonic mean formula (see e.g. Eymard et al. 2000).

$$c\left(\left(u_{K^\ell}^n,v_{K^\ell}^n\right);\left(u_{L^\ell}^n,v_{L^\ell}^n\right)\right):=\frac{2c_{K^\ell}^nc_{L^\ell}^n}{c_{K^\ell}^n+c_{L^\ell}^n}. \tag{12}$$

We note that (12) is consistent in the sense that $c((u,v);(u,v))=c(u,v)$.

Even though scheme A looks reasonable, it is not conservative. For the discretization of conservation laws, it is well known that a non-conservative discretization might converge to a wrong solution (see e.g. Hayes & LeFloch 1998). For non-conservative equations a possible remedy is the formulation of path-conservative schemes (Castro et al. 2006, Parés 2006). For parabolic equations (as treated here) there is a similar situation, which demands a careful consideration. In Bürger et al. 2000, Figure 2, it is demonstrated that a non-conservative discretization of the parabolic term

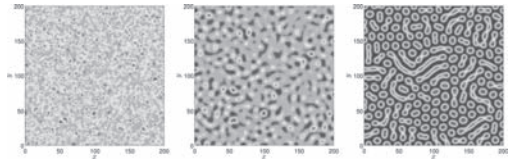

Figure 2. Numerical solution for the susceptible species u (top) and leaves of the corresponding tree data structure (bottom) at time instants $t=10$, $t=100$ and $t=1500$ (Example 1).

can produce spurious solutions; our scheme A is a two-dimensional version of the nonconservative discretization specified in their formula (12). Therefore, we try to mimic in scheme B the conservative discretization, see e.g. their formula (13). In other words, scheme B avoids averaged transmission coefficients, instead finite differences are calculated in terms of the antiderivatives A,B,C,

$$\frac{\partial A(u)}{\partial u}=a(u),\quad \frac{\partial B(v)}{\partial v}=b(v),$$
$$\frac{\partial C(u,v)}{\partial v}=c(u,v),$$

that retain the local nonlinear properties. Differencing with respect to these antiderivatives gives to the resulting scheme a conservative form. Scheme B has the form

$$\left|K^\ell\right|\frac{u_{K^\ell}^{n+1}-u_{K^\ell}^n}{\Delta t}=\left|K^\ell\right|f_{K^\ell}^n+$$
$$\sum_{\sigma\in\varepsilon_{\text{int}}\left(K^\ell\right)}\frac{\left|\sigma\left(K^\ell,L^\ell\right)\right|}{d\left(K^\ell,L^\ell\right)}\left\{\left(A_{L^\ell}^n-A_{K^\ell}^n\right)+\left(C_{L^\ell}^n-C_{K^\ell}^n\right)\right\},$$
$$\left|K^\ell\right|\frac{v_{K^\ell}^{n+1}-v_{K^\ell}^n}{\Delta t}=\left|K^\ell\right|g_{K^\ell}^n+ \tag{13}$$
$$\sum_{\sigma\in\varepsilon_{\text{int}}\left(K^\ell\right)}\frac{\left|\sigma\left(K^\ell,L^\ell\right)\right|}{d\left(K^\ell,L^\ell\right)}\left(B_{L^\ell}^n-B_{K^\ell}^n\right),$$

with $A_{K^\ell}^n:=A\left(u_{K^\ell}^n\right)$, $A_{L^\ell}^n:=A\left(u_{L^\ell}^n\right)$, $B_{K^\ell}^n:=B\left(u_{K^\ell}^n\right)$, $B_{L^\ell}^n:=B\left(u_{L^\ell}^n\right)$ which is justified due to the equalities

$$\Delta A(u)=a(u)\Delta u,\quad \Delta B(v)=b(v)\Delta v.$$

With respect to the definition of the coefficient C, there is the difficulty that

$$\nabla C=\frac{\partial C}{\partial u}\Delta u+\frac{\partial C}{\partial v}\Delta v,$$

i.e. there remains the unresolvable term $\frac{\partial C}{\partial u}\nabla u$. Therefore a semi-averaged form of $C^n_{K^\ell}$ is built as

$$C^n_{K^\ell} := C\left(\overline{u}, v^n_{K^\ell}\right), \quad C^n_{L^\ell} := C\left(\overline{u}, v^n_{L^\ell}\right),$$
$$\overline{u} = \overline{u}_{L^\ell K^\ell} = \frac{u^n_{L^\ell} + u^n_{K^\ell}}{2}.$$

The antiderivative of $c(u,v)$ as defined in (8) with respect to the variable v is calculated as

$$C(u,v) = c_0 u \tilde{v}^2 \left[(c_1 - u)/2 - \tilde{v}/3\right],$$

with $\tilde{v} = \min(v, c_1 - u)$. Scheme B should be more accurate than scheme A since the nonlinear functions are better approximated; more information is retained when differencing instead of simply calculating averages. For linear coefficient functions, when

$$A^n_{K^\ell} := a_0 u^n_{K^\ell}, \quad B^n_{K^\ell} := b_0 u^n_{K^\ell}, \quad C^n_{K^\ell} := c_0 u^n_{K^\ell},$$

both schemes (11) and (13) are the same and reduce to (10).

4 EXAMPLES

In Example 1, Model 1 is simulated, where the parameters are chosen according to Sun et al. 2009. The simulation is performed using a Cartesian mesh of $N = 262{,}144$ control volumes in the highest resolution level $H = 9$ and the time stepping is explicit with fixed time step $\Delta t = 0.01$. The model parameters are set to $K = 1000$, $\beta = 0.5$, and the constant self—and cross-diffusion coefficients are chosen to be $a_0 = 0.1$, $b_0 = 2$, $c_0 = 0.02$. The reference tolerance for the multiresolution algorithm is $\varepsilon_R = 0.001$. As initial data we assume that the density of both species is a random perturbation around the endemic stationary state (u^*, v^*). That is,

$$u(x,0) = u^* + u(x)\delta, v(x,0) = v^* + v(x)\delta, \quad x \in \Omega,$$

where $w(x)_\delta \in [0, 1]$ is a normally distributed variable, $w \in \{u, v\}$. In this contribution, two examples for the linear diffusion model are shown, in Berres & Ruiz-Baier 2011 there are two more examples. For Example 1 we set $d = 0.25$, $r = 0.27$, which gives (u^*, v^*) = (74.0741, 74.0741). The computational domain for Example 1 is the square $\Omega = (0, 200)^2$.

In Figure 2 In Example 1, "islands" of high concentration of susceptible individuals are formed. This reflects the phase separation triggered by the susceptible species avoiding the infected species.

In Example 2, Model 2 is simulated, where the parameters for the reaction equation are the same as in Example 1. The parameters for Model 2 are calibrated such that they quantitatively recover the orders of magnitudes of Model 1. More specifically we choose $a_0 = 0.5$, $b_0 = 3$, $c_1 = 3u^*$,

$$c_0 = 0.02\left(u^* v^* \left(c_1 - u^* - v^*\right)\right)^{-1},$$

and the remaining parameters as in Example 1. The initial condition is now

$$u(x,0) = u^* + \rho u_\delta, v(x,0) = v^* + \rho v_\delta \quad x \in \Omega,$$

where $\rho = 1\text{e}{-4}$.

From Figure 3 the result of a qualitative comparison between Schemes A and B for Model 2 is given; we also notice that the solution recovers the same scaling as in Example 1.We have computed a numerical solution of a one-dimensional problem using both schemes with a maximal resolution of 512 control volumes. Even though scheme A is based on a nonconservative discretization, one can see that the two solutions are almost indistinguishable. On the other hand, in terms of computational effort, scheme B has found to be more efficient than scheme A. Therefore, the numerical solution for the two-dimensional case has been computed using scheme B enhanced with the multiresolution strategy. In this setting, we also observe the formation of spatial patterns (see Figure 4). Notice however, that in contrast with the results related to Model 1, here the "islands" of high concentration values of the susceptible species are surrounded by a layer of low concentration values (also noticeable from Figure 3). This behavior is in well accordance with previous contributions in the field of

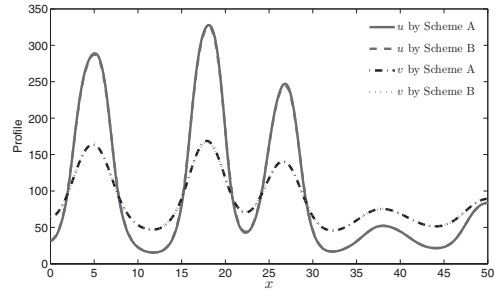

Figure 3. Profile of numerical solutions (species u) at time instant $t = 750$ obtained by the one-level finite volume schemes A and B (Example 2).

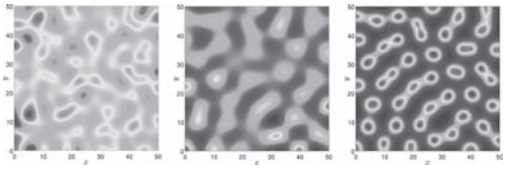

Figure 4. Numerical solution for u (top) and leaves of the corresponding tree data structure (bottom) at time instants $t = 50$, $t = 250$ and $t = 750$ (Example 2).

numerical simulation of cross-diffusion systems (see e.g. Andreianov et al. 2011, Galiano et al. 2003, Gambino et al. 2009).

5 CONCLUSIONS

This contribution is a condensed version of Berres & Ruiz-Baier 2011, where an efficient multiresolution method for the simulation of a nonlinear crossdiffusion model for epidemic dynamics is proposed. The ordinary differential equations involving the proposed reaction terms of our epidemic model are asymptotically stable in the sense that if the initial data are chosen close to the equilibrium then the solution converges to the equilibrium. The numerical examples of the two-dimensional reaction-diffusion equation show that there is a spatial phase separation in spite of the convergence behavior of the pure reaction terms. This means that the cross-diffusion in the parabolic terms of the reaction-diffusion equation is "stronger" than the attraction of the reaction terms. This is a remarkable property in comparison to other cross-diffusion models where the ordinary differential equations represented by the reaction part only show Lyapunov stability in the sense that initial data chosen in a close neighborhood of the equilibrium then the solution remains in this neighborhood.

For the simulation both a conservative and a non-conservative discretization have been proposed; both produce the same limit solution. The proposed schemes work stable both for the linear and nonlinear equations. The fully adaptive numerical method is particularly efficient to resolve phase interfaces due to the adaptive strategy.

From the numerical viewpoint, possible straightforward improvements include the use of time adaptive strategies such as local time stepping or Runge-Kutta-Fehlberg methods (Bendahmane et al. 2009a), or the use of a multiresolution analysis defined on general unstructured meshes.

From the model point of view one further issue is to choose different reaction kinetics in order study quantitatively how the pattern formation produced by the cross-diffusion term can be compensated by a stronger asymptotical stability of the reaction ODEs.

ACKNOWLEDGEMENTS

The first author is supported by Conicyt (Chile) through Fondecyt project #1120587. The work of the second author is supported by the European Research Council Advanced Grant "Mathcard, Mathematical Modelling and Simulation of the Cardiovascular System", Project ERC-2008-AdG 227058.

REFERENCES

Andreianov, B. Bendahmane, M. Ruiz-Baier, R. 2011. Analysis of a finite volume method for a crossdiffusion model in population dynamics. *Math. Meth. Models Appl. Sci*. 21: 307–344.

Badraoui, S. 2002. Existence of global solutions for systems of reaction-diffusion equations on unbounded domains. *Electron. J. Diff. Eqn*. 2002: 1–10.

Badraoui, S. 2006. Asymptotic behavior of solutions to a 2×2 reaction-diffusion system with a cross diffusion matrix on unbounded domains. *Electron. J. Diff. Eqn*. 2006: 1–13.

Barrett, J.W. & Blowey J.F. 2004. Finite element approximation of a nonlinear cross-diffusion population model. *Numer. Math*. 98: 195–221.

Bendahmane, M. B¨urger, R. Ruiz-Baier, R. Schneider, K. 2009a. Adaptive multiresolution schemes with local time stepping for two-dimensional degenerate reaction-diffusion systems. *Appl. Numer. Math*. 59: 1668–1692.

Bendahmane, M. Lepoutre, T. Marrocco, A. Perthame, B. 2009b. Conservative cross diffusions and pattern formation through relaxation. *J. Math. Pures Appl*. 92: 651–667.

Bendahmane, M. & Sepúlveda, M. 2009. Convergence of a finite volume scheme for nonlocal reaction-diffusion systems modelling an epidemic disease. *Disc. Cont. Dynam. Syst. - Series B 11*: 823–853.

Berres, S. Bürger, R. Frid, H. 2006. Neumann problems for quasi-linear parabolic systems modeling polydisperse suspensions. *SIAM J. Math. Anal*. 38: 557–573.

Berres, S. & Ruiz-Baier, R. 2011. A fully adaptive numerical approximation for a two-dimensional epidemic model with nonlinear cross-diffusion. *Nonlinear Anal., Real World Appl*. 12: 2888–2903.

Bürger, R. Evje, S. Karlsen, K.H. Lie, K.-A 2000. Numerical methods for the simulation of the settling of flocculated suspensions. *Chem. Eng. J*. 80: 91–104.

Bürger & R. Ruiz-Baier, R. 2009. Multiresolution simulation of reaction-diffusion systems with strong degeneracy. *Bol. Soc. Esp. Mat. Apl. S*ēMA 47: 73–80.

Bürger, R. Ruiz-Baier, R. Schneider, K. 2010. Adaptive multiresolution methods for the simulation of waves in excitable media. *J. Sci. Comput*. 43: 261–290.

Bürger, R. Ruiz-Baier, R. Schneider, K. Sepúlveda, M. 2008. Fully adaptive multiresolution schemes for strongly degenerate parabolic equations in one space dimension. *M2 AN Math. Model. Numer. Anal*. 42: 535–563.

Castro, M.J. Gallardo, J.M. Parés, C. 2006. High-order finite volume schemes based on reconstruction of states for solving hyperbolic systems with nonconservative products. Applications to shallow-water systems. *Math. Comp*. 75: 1103–1134.

Crandall, M. Pazy, A. Tartar, L. 1987. Global existence and boundedness in reaction-diffusion systems. *SIAM J. Math. Anal*. 18: 744–761.

Daddiouaissa, E.H. 2008. Existence of global solutions for a system of reaction-diffusion equations having a triangular matrix. *Electron. J. Diff. Eqn*. 2008: 141.

Eymard, R. Gallouët, T. Herbin, R. 2000. *Finite Volume Methods*. In: P.G. Ciarlet, J.L. Lions (eds.), Handbook of Numerical Analysis, vol. VII, North-Holland, Amsterdam: 713–1020.

Frid H. & Shelukhin, V. 2004. A quasi-linear parabolic system for three-phase capillary flow in porous media. *SIAM J. Math. Anal.* 35: 1029–1041.

Frid, H. & Shelukhin, V. 2005. Initial boundary value problems for a quasi-linear parabolic system in three-phase capillary flow in porous media. *SIAM J. Math. Anal.* 36: 1407–1425.

Galiano, G. Garzón, M.L. Jüngel, A. 2003. Semi-discretization and numerical convergence of a nonlinear cross-diffusion population model. *Numer. Math.* 93: 655–673.

Gambino, G. Lombardo, M.C. Sammartino, M. 2009. A velocity-diffusion method for a Lotka-Volterra system with nonlinear cross and self-diffusion. *Appl. Num. Math.* 59: 1059–1074.

Hayes, B.T. and LeFloch, P.G. 1998. Non classical shocks and kinetic relations: Finite difference schemes. *SIAM J. Numer. Anal.* 35: 2169–2194.

He, D. and Stone, L. 2003. Spatio-temporal synchronization of recurrent epidemics. *Proc. Roy. Soc. Lond. B* 270: 1519–1526.

Kermack, W.O. & McKendrick A.G. 1927. A contribution to the mathematical theory of epidemics. *Proc. Roy. Soc. Lond. A* 115: 700–721.

Kim, K.I. Lin, Z. Zhang, L. 2010. Avian-human influenza epidemic model with diffusion. *Nonl. Anal.: Real World Appl.* 11: 313–322.

Li, J. & Zou, X. 2009. Modeling spatial spread of infectious diseases with a fixed latent period in a spatially continuous domain. *Bull. Math. Biol.* 71: 2048–2079.

Li, K. Small, M. Zhang, H. Fu, X. 2010. Epidemic outbreaks on networks with effective contacts. *Nonl. Anal.: Real World Appl.* 11: 1017–1025.

Liu, J. & Zhang, T. 2010. Analysis of a nonautonomous epidemic model with density dependent birth rate. *Appl. Math. Model.* 34: 866–877.

Milner, F.A. & Zhao, R. 2008. S-I-R model with directed spatial diffusion. *Math. Popul. Stud.* 15: 160–181.

Müller, S. 2003. Adaptive Multiscale Schemes for Conservation Laws. Berlin: Springer-Verlag.

Ni, W.-M. 2004. Diffusion and cross-diffusion in pattern formation. *Rend. Mat. Acc. Lincei* 15: 197–214.

Parés, C. 2006. Numerical methods for nonconservative hyperbolic systems: A theoretical framework. *SIAM J. Numer. Anal.* 44: 300–321.

Phongthanapanich, S. & Dechaumphai, P. 2009. Finite volume element method for analysis of unsteady reaction-diffusion problems. *Acta Mech. Sin.* 25: 481–489.

Sun, G.-Q. Jin, Z. Liu, Q.-X. Li, L. 2009. Spatial pattern in an epidemic system with cross-diffusion of the susceptible. *J. Biol. Syst.* 17: 141–152.

Tian, C. Lin, Zh. Pedersen, M. 2010. Instability induced by cross-diffusion in reaction-diffusion systems. *Nonl. Anal.: Real World Appl.* 11: 1036–1045.

Webb, G. 1981. A reaction-diffusion model for a deterministic diffusive epidemic. *J. Math. Anal. Appl.* 84: 150–161.

Wong, J.C. 2008. The Galerkin finite element method for the solution of some spatio-temporally dependent reaction-diffusion systems. *Appl. Numer. Math.* 58: 352–375.